Research Article

Konstantinos Karvanis*, Soňa Rusnáková, Ondřej Krejčí, and Alena Kalendová

Thermal analysis of postcured aramid fiber/epoxy composites

https://doi.org/10.1515/rams-2021-0036
received March 20, 2021; accepted May 15, 2021

Abstract: In this study, aramid fiber-reinforced polymer (AFRP) composites were prepared and then postcured under specific heating/cooling rates. By dynamic mechanical analysis, the viscoelastic properties of the AFRP composites at elevated temperatures and under various frequencies were determined. Thermomechanical analysis (TMA), in the modes of creep-recovery and stress–relaxation tests, was also performed. Furthermore, differential scanning calorimetry was also used, and the decomposition of the AFRP composites, aramid fibers, and pure postcured epoxy, in two different atmospheres, namely, air atmosphere and nitrogen (N_2) atmosphere, was explored by the thermogravimetric analysis (TGA). From this point of view, the aramid fibers showed remarkably thermal resistance, in N_2 atmosphere, and the volume fraction of fibers (Φ_f) was calculated to be $\Phi_f = 51\%$. In the TGA experiments, the postcured AFRP composites showed very good thermal resistance, both in air and N_2 atmosphere, and this characteristic in conjunction with their relatively high T_g, which is in the range of 85–95°C, depending on the frequency and the determination method, classifies these composites as potential materials in applications where the resistance in high temperatures is a required characteristic.

Keywords: aramid fiber, epoxy, FRP, post-cure, thermal analysis

*** Corresponding author: Konstantinos Karvanis,** Department of Production Engineering, Faculty of Technology, Tomas Bata University in Zlin, Vavrečkova 275, 760 01, Zlin, Czech Republic, e-mail: karvanis@utb.cz
Soňa Rusnáková: Department of Production Engineering, Faculty of Technology, Tomas Bata University in Zlin, Vavrečkova 275, 760 01, Zlin, Czech Republic
Ondřej Krejčí, Alena Kalendová: Department of Polymer Engineering, Faculty of Technology, Tomas Bata University in Zlin, Vavrečkova 275, 760 01, Zlin, Czech Republic

1 Introduction

Nowadays, fiber-reinforced polymer (FRP) composites are widely used due to their superior properties such as high strength, high modulus, and anticorrosion resistance. These composites consist of fibers embedded in a polymer matrix. The low cost, the facile processability, the significant chemical resistance, and the low specific gravity are the principal advantages of a polymer matrix [1].

Several methods are used for the production of FRP composites, of which infusion is the most familiar technique. The pressure difference between the resin supply and the vacuum bag (cavity) is the axiom of the infusion techniques [2]. It is worthy of mention that characteristics of the polymer composites rely on the techniques of the material processing and as well as on the nature and properties of their constituents [3].

As the artificial fibers have much better thermal resistance than the polymer matrix, the introduction of them, in a percentage of more than 50% in an FRP composite, is of great interest. In particular, because the glass transition (α-transition) temperature of most polymer amorphous matrices is low compared to one of the reinforcement phases, the viscoelastic behavior of polymer-based composites is defined by matrix properties [4].

Improving the thermal behavior of the FRP composites is always a major goal for polymer researchers, especially with low-cost techniques, such as the post-cure process. In this technique, the FRP composites, after their curing, are exposed to high temperatures, usually in an oven, under specific heating–cooling rates.

It should be noted that with curing at room temperature, complete cross-linking is not achieved frequently, so such cold-cured pieces are usually exposed to post-cure under elevated temperatures [5]. Furthermore, through the curing process, polymers are converted from viscoelastic fluids to viscoelastic solids [6].

Thermal analysis is the study of the effect of the temperature on the properties of materials, and it involves techniques such as the dynamic mechanical analysis

(DMA), TMA, thermogravimetric analysis (TGA), and differential scanning calorimetry (DSC). The importance of the DMA becomes remarkably significant especially for the FRP composites, which in their real-life applications are exposed to different environmental factors including variations of temperature and loads. Generally, by thermal analysis, the degree of the polymers' cure can be explored. Remarkably, the cross-linking network is continuously growing during the curing, so the glass transition of thermosetting polymer matrices is in strong correlation with the degree of the cure [7].

Epoxy resins are widely used as polymer matrices and especially in high demanding applications, where good properties and low weight are essential characteristics. It is also worthy of mention that the mechanical properties of epoxy resins are better than those of polyesters and vinyl esters and that in aerospace composites, the mainly used thermoset polymer matrix is the epoxy [8]. In applications where high properties are essential, such as in the advance composites industry, one of the most widely used fibers is the aramid. The aramid fibers are organic and have low densities and superior toughness [9]. It must be noted that the Kevlar® does not melt [10].

Creep, stress–relaxation, and dynamic response to loads varying sinusoidally with the time experiments are frequently used for the determination of the viscoelastic response characteristics of the materials [11].

The superior properties of aramid fibers have led the researchers to explore them in combinations with different polymer matrices and under various experimental circumstances. Karahan et al. [12] studied the ballistic performance of hybrid panels that were prepared by woven and unidirectional para-aramid fabrics. By using three different types of matrices, Yeung and Rao [13] fabricated three different types of Kevlar-49 fiber-reinforced thermoplastic composites, and they determined the tensile strength, compressive strength, flexural strength, and flexural modulus of them. Also, in this study, the micromechanical-based models, rule of mixtures, inverse rule of mixtures (IROM), Halpin Tsai, and Xu Reifsnider were used for the theoretical prediction of the mechanical properties of composites. By a comparison between experimental and theoretical predictions, it was revealed that the model of Xu and Reifsnider predicted quite accurately the compressive strength of the composites, whereas the theoretical predictions, through the IROM model, for the flexural strength of the composites, were around 15% higher than the experimental [13].

In the author's previous research work [14], the effect of the orientation of unidirectional glass fibers in the longitudinal or transverse direction and woven glass fibers at 0° (fibers at 0°/90°) or at 45° (fibers at −45°/+45°) in epoxy matrix composites was investigated. In this study, through the vacuum bag oven method and by using prepreg materials, ten kinds of glass or carbon fiber-reinforced epoxy composites were fabricated. The results revealed that the unidirectional glass fibers when they are placed in the longitudinal direction contribute toward the epoxy matrix composite to exhibit higher storage modulus and loss modulus than if they are placed in the transverse direction, and that as the volume fraction of glass fibers in an epoxy matrix composite increases, these composites exhibit higher storage and loss modulus [14].

Qian et al. [15] produced aramid fabric-reinforced polyamide composites and investigated their out-of-plane compression properties, in the strain rate of 400–1,200 s^{-1}, and also their quasi-static properties.

The tensile behavior of aramid –fiber-reinforced polymer (AFRP) at different strain rates (25, 50, 100, and 200 s^{-1}) and temperatures (−25, 0, 25, 50, and 100°C) was explored by Zhang et al. [16]. Sethi and Ray [17] studied the effect of liquid nitrogen (LN_2) temperature on the interlaminar shear strength of woven fabric Kevlar/epoxy composites at different loading speeds (1, 10, 100, 200, and 500 mm·min^{-1}). In particular, the composites were prepared by the hand layup technique, investigated through short-beam shear tests, and also characterized by the scanning electron microscopy [17]. The mechanical, dynamic, and rheological properties of a short Twaron aramid fiber-reinforced thermoplastic polyurethane, with varying percentages of fibers (0–30 wt%), were explored by Akbarian et al. [18]. Moreover, a scanning electron microscope was used for the investigation of the tensile and cryo-fracture fracture surfaces of these composites [18].

However, it seems that a research study, investigating in depth and with various thermal analysis methods, on postcured aramid fiber-reinforced epoxy composites and especially the effect of the post-cure process is missing. Most of the research works, about the thermal analysis of AFRP composites, concentrate usually on no more than two techniques of this sector, whereas the postcured FRP composites, due to its viscoelastic matrix, must be explored through several thermal analysis techniques, and hence their T_g, viscoelastic properties and thermal decomposition behavior to be investigated in depth. So, despite the fact that many research studies have been presented about the thermal analysis of postcured FRP composites; conversely, there are many details, which need further investigation and improvement.

In this study, through the vacuum infusion process (VIP), eight-layered AFRP composites, composed of twill 2/2 weave aramid fabric, were prepared and then

postcured under specific heating/cooling rates. By DSC in N_2 atmosphere, these composites were explored in the range of 30–600°C, whereas by DMA, their dynamic mechanical properties in terms of storage modulus, loss modulus, and tan δ, in the temperature range of 30–200°C and at 1, 5, and 10 Hz were determined. Moreover, based on the DSC curves and the peak values of loss modulus and tan δ curves, T_g of the AFRP composites was defined, whereas TMA was also performed in the modes of creep-recovery and stress–relaxation experiments. Furthermore, through TGA, the weight variation of the AFRP composites, aramid fibers, and pure postcured epoxy, as a function of the temperature, in two different atmospheres, namely, air atmosphere and nitrogen atmosphere, was recorded, and as well as the volume fraction (Φ_f) of the aramid fibers in the composite structure was calculated.

2 Experimental

2.1 Materials

For the preparation of the AFRP composites, the Style 502 aramid fibers fabric, produced from the company C. Cramer & Co (Heek, Germany), with 161 g·m^{-2} dry weight, twill 2/2 weave, and consisting of the fibers Kevlar® 49 T965 (1580dtex) (DuPont™) was used. Moreover, the polymer matrix is a mixture, in parts by weight 100:30, of the epoxy resin Biresin® CR80 and the hardener Biresin® CH80-2, both fabricated from Sika® (Baar, Switzerland). The mixture [19] of Biresin® CR80 and Biresin® CH80-2 at 25°C has approximately viscosity of 350 mPa·s, whereas a fully cured neat piece of this resin and hardener has according to ISO 75A, heat distortion temperature of 89°C.

2.2 Preparation of the AFRP composites

For the production of the FRP composites, there are many variations of the VIP, with the differences between them to be indistinguishable, and based on the experience and the preferences of the according researcher to avoid confusion, in this study the production method of AFRP composites is named simply VIP, and special attention is given on the accurate description of it.

In details, a rectangular plate of glass, with dimensions of 90 mm × 62 mm × 10 mm (length × width × thickness), was used as the base of the vacuum system. To ensure a smooth surface, the upper part of this plate was polished three times with a wax. Next, eight layers of the aramid fabric were cut, with dimensions of 50 mm × 30 mm, and placed on the polished surface. In the next step, a peel ply and a perforated release film were placed over the fabrics' stacking, and then a resin flow medium was used so as to cover all of them.

Next, near and across the vertical sides of the fabrics, the resin distribution channels, including the infusion spiral medium flow and two t-fittings, one connected with the vacuum pump and the other with the resin supply, were placed. Finally, the whole system was closed with the vacuum bag, which was stuck across the perimeter of the glass with sealant tape and air leak test took part. Then, the vacuum pump was turned on and the resin, which was previously gently stirred until to achieve homogeneity, was infused in the mold through the supply tube. The composite plates were let for solidification, in the laboratory environment, at 23°C for 7 days, and then, they were postcured in an electric oven, which was modified with a PID controller, as suggested [19] by the producer of the resin, heating–cooling rates. It must be noted that the curing for 7 days at 23°C was chosen according to an example from the datasheet of the resin [19].

First, the temperature was increased, with a heating rate of 0.2°C·min^{-1}, from 23 to 80°C followed by an isothermal hold at 80°C for 9.5 h. Then, the cooling of the composites plates, from 80°C up to 23°C, took part with a cooling rate of 0.5°C·min^{-1}. Finally, the specimens were cut in the desired dimensions through the water jet tool (Figure 1). It is significant that, during the preparation of the AFRP composite plate, the weight of the eight aramid fiber fabric layers was measured and then compared with

Figure 1: AFRP composite specimens.

the final weight of the composite plate. It was found that the weight of the aramid fiber fabrics is approximately 54% of the AFRP composite plate.

2.3 Experiments

2.3.1 General experimental conditions

In all of the experiments, the specimens were stored in the laboratory environment at 23°C for not less than 40 h before the tests. Also, during the experiments, the conditions in the laboratory were at a temperature of 23°C and humidity of approximately 50%.

2.3.2 DMA, TMA creep-recovery, and TMA stress–relaxation experiments

The DMA, TMA creep-recovery, and TMA stress–relaxation experiments were performed by the instrument DMA 1, from METTLER TOLEDO (Schwerzenbach, Switzerland), under three-point bending configuration and with using the STARe Software. In particular, the specimens were of the rectangular shape with dimensions 40 mm × 5 mm × 1.75 mm. (length × width × thickness) with the span length, between the supports, to be 30 mm.

In particular, the DMA took part by scanning in the range 30–200°C, with a heating rate of 2°C·min^{-1}, at frequencies of 1, 5, and 10 Hz, with the displacement to be 15 μm, whereas 1 N force was used as preload.

The TMA creep-recovery experiments were exhibited at isothermal 25°C, with a force of 1, 3, or 5 N to be applied on the specimens for 30 min and then the recovery of them to be recorded under 0 N for 120 min; one more experiment of this kind was carried out at 50°C with an initial force of 1 N. During the stress–relaxation tests, 12 μm extension was applied on the AFRP composite specimen, at 25°C, and its time-dependent stress was being measured for 48 min.

2.3.3 TGA

The TGA experiments were performed with the instrument TGA Q50 from TA Instruments (New Castle, Delaware, USA). It must be noted that the TGA tests were set and performed using the Thermal Advantage Release 5.4.0 software, and the results were evaluated with the TA Instruments Universal Analysis 2000 version 4.5A program. Due to the fact that the TGA is of significant importance in the thermal analysis sector, various experiments were performed. In detail, TGA was performed as follows:

- The decomposition of pure postcured epoxy, aramid fibers, and AFRP composites, in the range 30–900°C, with the heating rate of 10°C·min^{-1}, in two different atmospheres, namely, air atmosphere and nitrogen atmosphere; in the latter atmosphere, two samples were tested, which were taken from different places of the AFRP composite plate so as to check the reliability of the production method.
- The thermal stability of aramid fibers, AFRP composite, and pure postcured matrix, in N_2 atmosphere, at isothermal 350°C for 240 min.
- To determine the maximum temperature at which aramid fibers are not thermally affected, TGA isothermal scans, in nitrogen atmosphere, were exhibited in the range of 360–380°C with every 60 min step of 10°C.

In all of the TGA scans, an alumina crucible was used for the placement of the specimens, and the total flow rate was adjusted to be 100 mL·min^{-1}, balance purge flow of 40 mL·min^{-1}, and sample purge flow of 60 mL·min^{-1}. It must be noted that AFRP composites were TGA tested with samples of 35 mg because their complex composite structure requires enough mass during its TGA exploration, whereas aramid fibers and epoxy matrix were TGA tested with samples of approximately 14–20 mg.

2.3.4 DSC

The DSC was carried out with the DSC 1 METTLER TOLEDO (Schwerzenbach, Switzerland) by scanning at 30–600°C with the heating rate of 20°C·min^{-1} in nitrogen atmosphere using STARe SW 14.00 software. In this experiment, the 23 mg sample was placed in the aluminum sample holder of 40 μL, and then, it was heated two times and cooled two times.

3 Results

3.1 DMA

The storage modulus (E') of the AFRP composites, over the range 30–200°C, at 1, 5, and 10 Hz, is presented in Figure 2. As can be seen, the storage modulus curves are

separated in three regions: 30–75°C is the glassy state, where the polymer molecules are rather frozen and the composite exhibits high storage modulus; 75–110°C is the middle transition region, correlated with T_g; and 110–200°C is the rubbery region. Noteworthy, at 1 and 5 Hz, the storage modulus is slightly reduced as the temperature increases in the glassy state region, and at 10 Hz, it is almost stable. This is due to the fact that the higher frequency contributes toward the elastic behavior to dominance over the viscous behavior in the polymer matrix, and thereby, the AFRP composite exhibits better thermal stability. The polymers over their glass transition, due to the fact that the mobilities of the main chain (segmental) and of the side groups are raised, have viscoelasticity, high mechanical damping, and low storage modulus [20]. Also, as the frequency is raised, the initial values of the storage modulus is reduced.

The energy that was dissipated as heat in every cycle of the sinusoidal deformation is correlated with loss modulus [21]. Figure 3 depicts the loss modulus (E'') of the AFRP composites at 30–200°C and at frequencies of 1, 5, and 10 Hz. In this graph, it is observed that at about 70°C, the loss modulus curves depict an abrupt increase, achieving maximum values, whereas then they fell sharply to almost zero values. It is important to emphasize that at the temperature range where the E'' achieves peak, the E' is reduced. This can be attributed to the fact that there is free movement in the polymeric chains at higher temperatures [22].

The tan δ is the ratio of loss modulus to storage modulus, and it provides a determination of the damping of materials [23]. Furthermore, higher tan δ indicates nonelastic behavior, whereas low tan δ is correlated with high elastic behavior of the materials [24]. Figure 4 shows the tan δ of the AFRP composites over the temperature range of 30–200°C at frequencies of 1, 5, and 10 Hz. As

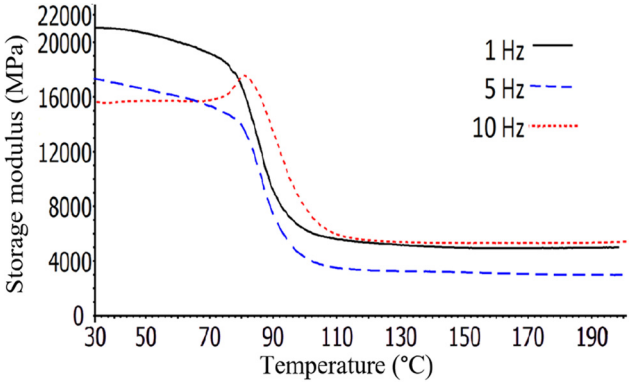

Figure 2: Storage modulus of the AFRP composites at 30–200°C and at 1, 5, and 10 Hz.

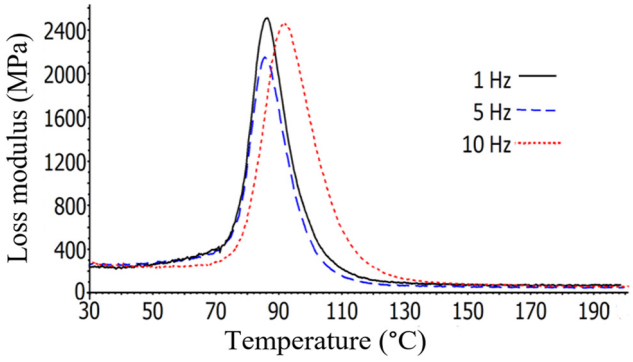

Figure 3: Loss modulus of AFRP composites at 30–200°C and at 1, 5, and 10 Hz.

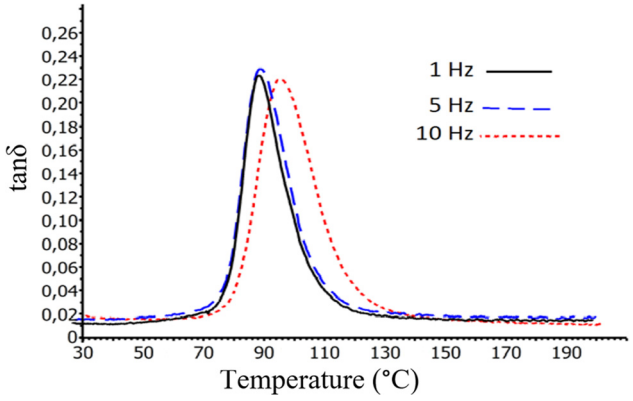

Figure 4: tan δ of the AFRP composite in the range of 30–200°C and at 1, 5, and 10 Hz.

can be seen, the tan δ values are relatively low and so it can be concluded that the elastic (solid-like) behavior dominates over the viscous behavior. Moreover, as the frequency is increased, the peak of the tan δ curves moves to higher temperatures. Remarkably, by the tan δ, the adhesion between fibers/polymer can be qualified. Probably, the specimen under continuous cyclic loading will dissipate energy at the fiber/matrix interface, and the amount of it relies on the degree of the adhesion [25]. So, a weak adhesive bond is expected to contribute to more energy loss, thus resulting in a higher damping coefficient [25]. In the case of the AFRP composites, tan δ = 0.22–0.23 and thus indicates that a very good adhesion bond has been formed between aramid fibers/epoxy.

3.2 Glass transition temperature T_g (°C)

At T_g, the polymer changes from a stiff glassy state to a pliant rubbery state [26]. Table 1 illustrates T_g of the AFRP

Table 1: T_g of the AFRP composites

AFRP composite	1 Hz	5 Hz	10 Hz
T_g (peak of loss modulus)	86.40°C	85.52°C	92.29°C
T_g (peak of tan δ)	88.07°C	88.39°C	95.10°C

composites, which were acquired from the corresponding temperatures of the peak of loss modulus and tan δ curves at 1, 5, and 10 Hz. The datasheet [27] of the producer of the resin/hardener, in the chapter "Detailed Information: Infusion and RTM System," refers to the combination of Biresin® CR80 and Biresin® CH80-2, T_g = 92°C. So, the AFRP composites are characterized as fully cured; the cure–postcure process that was followed is highly effective for the production of the particular materials.

Furthermore, it can be noticed that between 1 and 5 Hz, T_g remains almost stable or reduced very slightly, and at 10 Hz, it is highly increased, and that T_g that was acquired from the tan δ is higher than the that is determined by the loss modulus curves.

3.3 TMA creep-recovery and TMA stress–relaxation tests

The AFRP composites' creep-recovery behavior is shown in Figure 5. As can be seen, the final deformation (plastic), caused by forces on the structure of composites is very small; the elastic behavior prevails entirely over the viscous behavior. A perfectly elastic material will recover to its primary dimension after the release of the force. Even in the five Newton stress tests, in which primarily high initial deformation was obtained in the structure of the specimens, the elastic recovery after the release of the force is remarkably high.

Furthermore, between a comparison of the creep-recovery tests at 25 and 50°C, the good resistance in deformation of the AFRP composites at elevated temperatures can be obtained; this is confirmed by the fact that the initial displacement caused by the 1 N is the same in both temperatures and that both curves are very similar. Despite the fact that as the initial forces are raised, the displacement in the structure of the composites is also increased, the creep resistance of the composites is notably high under all the experimental conditions; the creep behavior of the composites is almost stable during the first 30 min of these experiments. Moreover, the recovery occurred immediately after the release of the force.

Figure 6 depicts the stress–relaxation curve, under 12 μm extension for 48 min, of the AFRP composite. The viscoelastic behavior of the composite structure is notable in the first few minutes of this experiment as then the curve becomes almost stable (Figure 7).

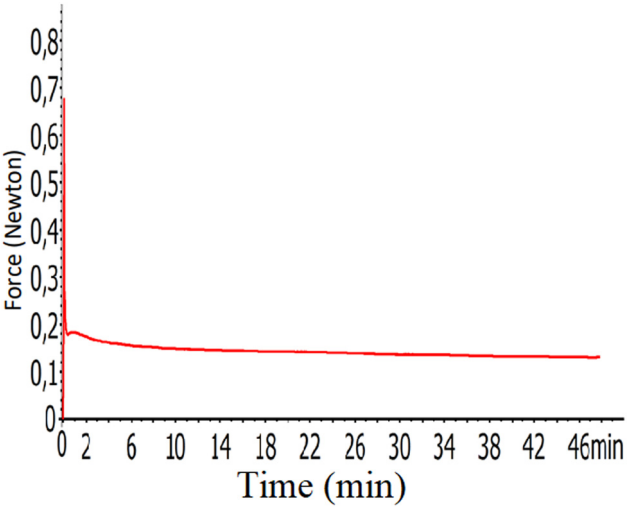

Figure 6: Stress–relaxation curve of the AFRP composite.

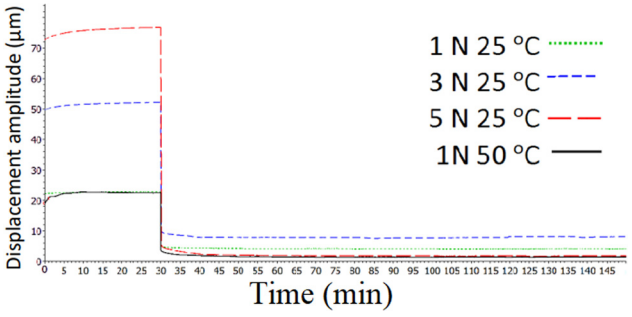

Figure 5: Creep-recovery of the AFRP composites.

Figure 7: Zoomed view of the stress–relaxation curve.

3.4 TGA

Figure 8 illustrates the weight variation of pure postcured epoxy and aramid fibers at 350°C for 240 min in nitrogen atmosphere. Based on these TGA curves, an approach for the determination of the Φ_f of the aramid fibers in the AFRP composites was considered. In detail, it was revealed that after exposure at 350°C for 240 min, in N_2, the postcured epoxy loses approximately 80% of its weight, whereas under the same circumstances, the aramid fibers remain mostly thermally unaffected; they lose only approximately 4.5% of their weight. The biggest part of this weight is attributed to the loss of humidity, which was concentrated on the surface of the fibers. The aramid fibers are highly hydrophilic; this is verified by the fact that after this small weight loss, the weight curve becomes linear and steady at 95.5%.

So, two samples, for reliability, of the AFRP composite were TGA tested (Figure 9). It was found that the remaining weight of them, after exposure for 240 min at 350°C, in N_2 atmosphere, is 66.65 and 63.27%, respectively. It must be noted that the overall time on the x-axis is more than 240 min because the instrument measures also the time as the temperature reaches 350°C. Afterward, with the use of simple mathematics, the remaining 20% of the epoxy, in the two AFRP composite samples, was withdrawn, and thus, $W_{f,1}$ = 58.32%, $W_{f,2}$ = 54.09%, and average $W_{f,1,2}$ = 56.20%.

Then, with the use of the following equation [28]:

$$\Phi_f = \frac{1}{1 + \frac{\rho_f}{\rho_m}\left(\frac{1}{w_t} - 1\right)}, \quad (1)$$

where Φ_f = volume fraction of fibers, Φ_m = volume fraction of matrix, ρ_m = density of matrix = 1.16 g·cm^{-3}, ρ_f = density of reinforcing phase = 1.44 g·cm^{-3}, and W_t = weight proportion of the reinforcing phase. So, finally, it was found that approximately Φ_f = 51%, and thus, Φ_m = 49%. It must be noted, that during the preparation of the composite laminates, the weight of the aramid fabric reinforcement was measured and then compared with the whole weight of the AFRP composite structure. It was found that the aramid fibers' fabrics consist approximately 54% of the whole weight of the AFRP composite. So, it is concluded that the experimentally determined W_t = 56.20% is very close to the realistic value.

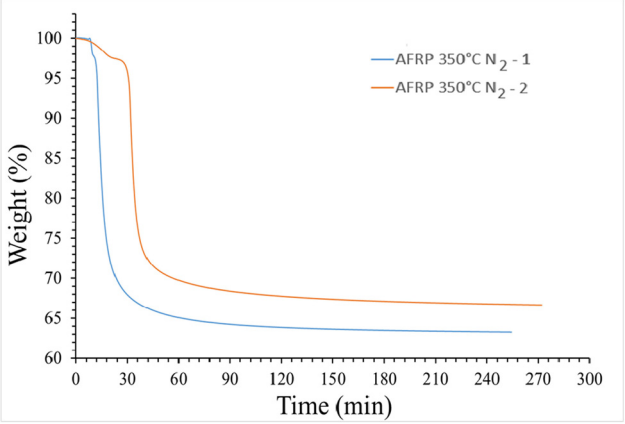

Figure 9: TGA of the AFRP composite (two samples) at 350°C for 240 min in N_2 atmosphere. The difference on the time axis is because these two samples were heated up to 350°C with different heating rates.

The isothermal TGA tests, with temperature steps after a particular time, are of great interest because they correlate the temperature with the time so the weight of the materials can be precisely determined simulating real-life applications. Figure 10 depicts the thermal behavior of the aramid fibers, in nitrogen atmosphere, in

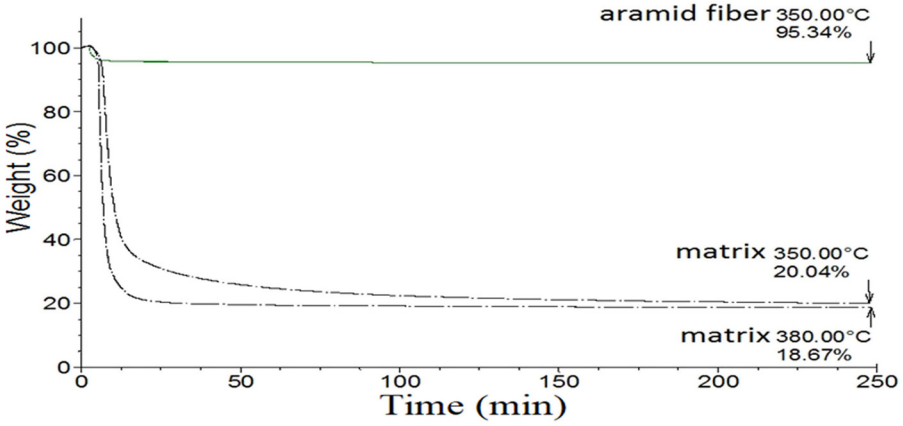

Figure 8: TGA graphs at 350°C for 240 min of —— aramid fiber, —·— pure postcured epoxy in N_2 atmosphere (epoxy also at 380°C).

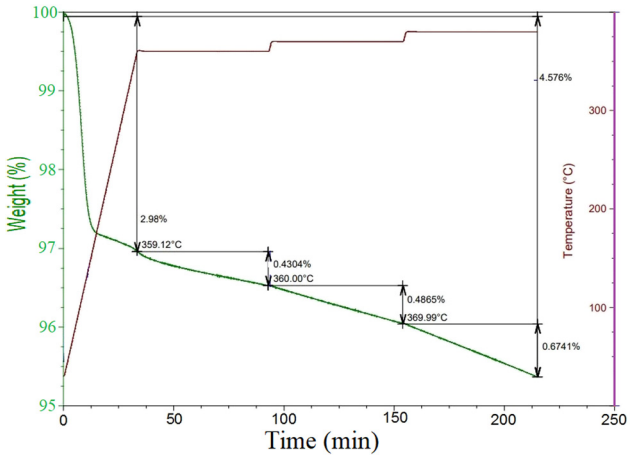

Figure 10: TGA isothermal scans of the aramid fibers at 360, 370, and 380°C, respectively, in N_2 atmosphere, with every 60 min step of 10°C.

isothermal scans at 360, 370, and 380°C, respectively, with every 60 min step of 10°C. The initial 3% weight reduction is attributed to humidity due to the hydrophilic character of these fibers. As can be seen, the aramid fibers show remarkably good thermal stability as they are slightly thermally influenced above 370°C.

Figure 11 illustrates the thermal decomposition of the AFRP composites, in the range of 30–900°C, in air and nitrogen atmospheres, respectively. As was expected, high Φ_f contributes toward the composite structure to achieve very good thermal resistance. Notably, under both atmospheres, the weight loss mainly occurs at 450°C. In the case of air atmosphere, the oxidation phenomenon leads to whole thermal degradation of the composites' weight up to 590°C, whereas under N_2 gas, where pyrolysis takes part, 30% of the composite weight remains up to the final temperature of 900°C. Moreover, to check the reliability of these experiments and of the VIP production method, two samples, which were taken from different places of the AFRP composite plate, were tested in N_2. Through this graph, the high reliability of the VIP production method is revealed. Despite the small size of the TGA specimens, each of 35 mg, both curves are very identical and concluding in the same remaining weight at the final 900°C. Thus, the composites' production method is characterized as highly effective.

Figure 12 depicts the corresponding DTG curves of Figure 11. In N_2 atmosphere, the first peak, at approximately 350°C, is dedicated to thermal decomposition of the matrix, whereas the second peak, at about 580°C, is a combination of thermal degradation of aramid fibers and the remaining part of the matrix.

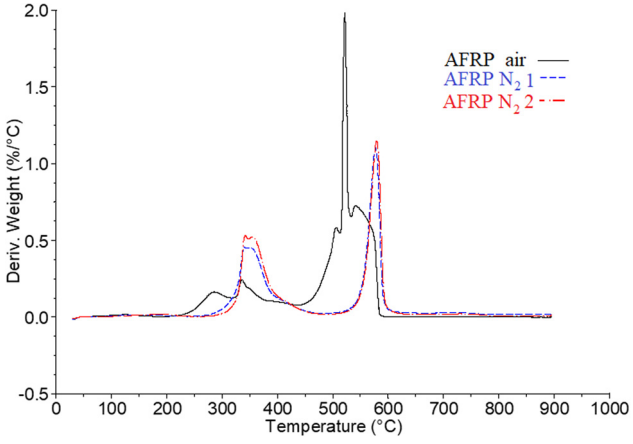

Figure 12: DTG (weight loss rate) of the AFRP composite in air and N_2 atmosphere, respectively.

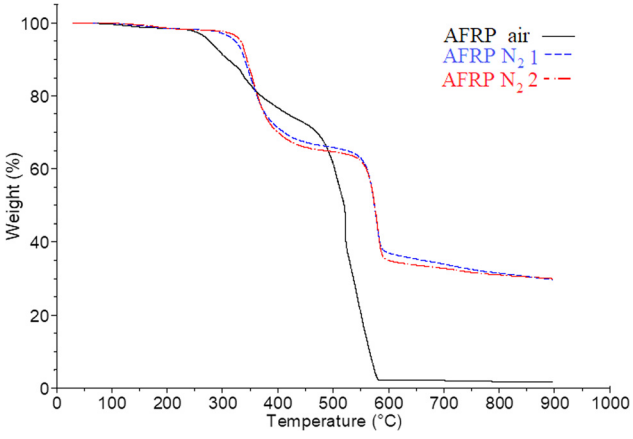

Figure 11: TGA results showing the weight (%) of the AFRP composites as a function of the temperature, in air and N_2 atmosphere, respectively.

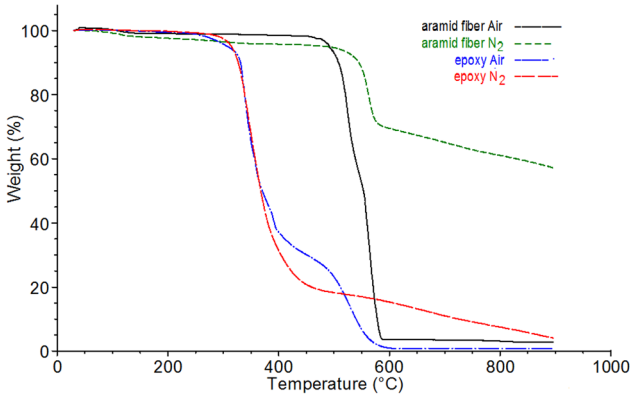

Figure 13: TGA results showing the weight (%) of the aramid fibers and pure post-cure epoxy matrix as a function of temperature in air and N_2 atmosphere, respectively.

Figure 13 presents the thermal degradation, in the temperature range 30–900°C, of pure cured epoxy and aramid fibers in air and N_2 atmospheres, respectively. The first obvious observation is that, at both atmospheres, the aramid fibers have much better thermal behavior than the epoxy; the aramid fibers are mainly thermally affected above the 480°C, whereas the postcured epoxy is highly thermally influenced over 275°C. The exposure of FRP composites around the resin decomposition temperature causes their organic matrix to decompose, releasing smoke, soot, heat, and toxic volatiles [29]. Moreover, both epoxy and aramid fibers, in air atmosphere, due to thermal oxidation, are completely thermally degraded up to 590°C.

3.5 DSC

Figure 14 shows the DSC curves at 30–600°C, of the two heating circles and the two corresponding cooling circles, of the AFRP composite. When the materials are subjected to a change in the physical state, like recrystallization or melting, or when they go through a chemical reaction, they discharge absorbed energy [30]. The enthalpy variations that take part during these transitions are measured with a differential scanning calorimeter [30]. T_g can be determined through various ways with the most familiar of them being the onset and midpoint (inflection) temperature [31].

Based on the datasheet [19] of the manufacturer of the resin-hardener, T_g of a fully cured neat resin (Biresin® CR80 and Biresin® CH80-2), determined according to the standard ISO 11375, is 93°C. This standard specifies T_g using DSC experiments, but the author of this study did not specify T_g according to this standard. However, T_g determined from the midpoint of the first heating is 94.67°C, a value that cannot be compared directly with the one from the datasheet, but, on the other hand, it must be noted that both that were determined by DSC are very close.

As general information about various T_g values, determined by DSC experiments under nitrogen atmosphere, of cold-cured epoxies, an epoxy adhesive [32] that was cured for 3.5 months at 23°C achieved T_g = 57.1 ± 0.4°C and a commercial medium density epoxy resin [33] that was cured for 11 months at 20–23°C exhibited approximately T_g = 60°C. It seems that the post-cure process contributes toward the fast and upgraded curing of epoxy.

4 Conclusion

In this study, AFRP composites, with twill 2/2 weave fabric, were fabricated and explored through various thermal analysis methods. In particular, these composites after their 7 days curing at room temperature were postcured in an electric oven under specific heating and

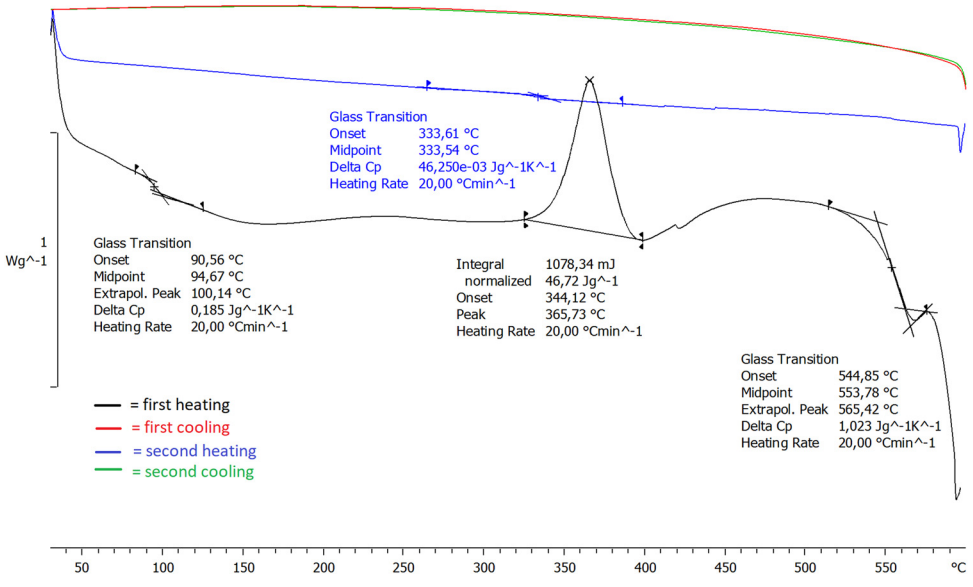

Figure 14: DSC of the AFRP composite.

cooling rates. Through the TGA experiments, it was revealed that the thermal degradation in an oxidative environment (i.e., in air atmosphere) is much more harmful than the one due to pyrolysis (in N_2). This is verified from the fact that all the materials, aramid fibers, AFRP composite, and pure postcured epoxy in air atmosphere have completely thermally degraded up to 590°C. Notably, at 480–600°C, the aramid fibers and AFRP composites lost the biggest part of their weight at a very rapid rate.

The experimentally determined T_g values are in agreement with those from the datasheets of the resin producer, the fact that verifies that the AFRP composites are fully and appropriately cured; the cure–postcure process, which was followed, is highly effective for these kinds of materials. It must be noted that the glass transition is mostly a temperature range where the properties of the materials are excessively affected than a specific temperature. In particular, the remarkably high T_g of the AFRP composites makes them a safe choice in everyday applications such as body parts of exclusive cars and motorcycles, athletic equipment, and racing helmets.

In addition, the controlled conditions of the production method contribute positively to the production of composites with predictable properties, the factor that is of significant importance in the advanced FRP composites industry. Furthermore, the low density of the aramid fibers, 1.44 $g{\cdot}cm^{-3}$, results in a composite structure with low weight, thus making the composite highly attractive in a broad range of applications and especially in the airplane industry, where, nowadays, the efforts for fuel savings are of significant importance.

Notably, through the TMA creep-recovery experiments, it was observed that the recovery of the composites took part immediately after the release of the force and that in all cases the final (plastic) deformation in the structure of the AFRP composites is relatively small. Relating this aspect, with the overall results from the DMA experiments, it can be concluded that, at T_g, the elastic behavior prevails entirely over the viscous behavior in the structure of AFRP composites. Moreover, the creep-recovery behavior of the composite was found to be the same at 25–50°C, confirming the ability of the AFRP composite structure to work in this temperature range.

Acknowledgments: This work and the project is realized with the financial support of the internal grant of TBU in Zlin No. IGA/FT/2021/006 funded from the resources of specific university research.

Funding information: This work and the project are realized with the financial support of the internal grant of TBU in Zlin No. IGA/FT/2021/006 funded from the resources of specific university research.

Author contributions: Investigation, methodology, preparation of composite samples, software, supervision, visualization, writing manuscript, writing – review and editing, K.K.; investigation, resources, funding acquisition, software, S.R.; investigation, software, O.K.; investigation, software, A.K. All authors have discussed and agreed to the published version of the manuscript.

Conflict of interest: The authors state no conflict of interest.

References

[1] Thomas, S., K. Joseph, S. K. Malhotra, K. Goda, and M. S. Streekala. *Polymer composites*, Vol. 1, 1st edn, Wiley-VCH Verlag GmbH & Co. KgaA, Weinheim, 2012.
[2] Hindersmann, A. Confusion about infusion: An overview of infusion processes. *Composites Part A: Applied Science and Manufacturing*, Vol. 126, 2019, id. 105583.
[3] Ivanov, Y., V. Cheshkov, and M. Natova. *Polymer composite materials-interface phenomena and processes*, Kluwer Academic Publishers, The Netherlands, 2001.
[4] Katunin, A., W. Hufenbach, P. Kostka, and K. Holeczek. Frequency dependence of the self-heating effect in polymer-based composites. *Journal of Achievements in Materials and Manufacturing Engineering*, Vol. 41, No. 1–2, 2010, pp. 9–15.
[5] Ehrenstein, G. W. *Polymeric materials structure-properties-applications*, HANSER, Germany, 2001.
[6] Hossain, M. and P. Steinmann. Continuum physics of materials with time-dependent properties: Reviewing the case of polymer curing. In *Advances in applied mechanics*, Bordas S. P. A. and D. S. Balint, eds, Vol. 48, 1st edn, Elsevier, London, UK, 2015, pp. 141–259.
[7] Adams, D. F., L. A. Carlsson, and R. B. Pipes. Processing of composite laminates. *Experimental characterization of advanced composite materials*, 4th edn, CRC Press, Boca Raton, 2014, pp. 37–55.
[8] Saba, N. and M. Jawaid. Epoxy resin based hybrid polymer composites. In *Hybrid polymer composite materials: Properties and characterisation*, Thakur V. K., M. K. Thakur, and A. Pappu, eds, Woodhead Publishing, United Kingdom, 2017, pp. 57–82.
[9] Campbell, F. C. *Manufacture processes for advanced composites*. Elsevier Advanced Technology, UK, 2004.
[10] Kevlar® Aramid fiber technical guide. Copyright © 2017 DuPont.
[11] Roy, S. and J. N. Reddy. *Computational modeling of polymer composites: A study of creep and environmental effects*. CRC Press LLC, United States of America, 2013.
[12] Karahan, M., N. Karahan, M. A. Nasir, and Y. Nawab. Effect of structural hybridization on ballistic performance of aramid fabrics. *Journal of Thermoplastic Composite Materials*, Vol. 32, 2018, pp. 1–20.

[13] Yeung, K. H. and K. P. Rao. Mechanical properties of Kevlar-49 fibre reinforced thermoplastic composites. *Polymers and Polymer Composites*, Vol. 20, No. 5, 2012, pp. 411–424.
[14] Karvanis, K., S. Rusnakova, M. Žaludek, and A. Capka. Preparation and dynamic mechanical analysis of glass or carbon fiber/polymer composites. *IOP Conference Series: Materials Science and Engineering*, Vol. 362, 2018, p. 012005.
[15] Qian, X., H. Wang, D. Zhang, and G. Wen. High strain rate out-of-plane compression properties of aramid fabric reinforced polyamide composite. *Polymer Testing*, Vol. 53, 2016, pp. 314–322.
[16] Zhang, X., D. Zhu, Y. Yao, H. Zhang, B. Mobasher, and L. Huan. Experimental study of tensile behaviour of AFRP under different strain rates and temperatures. *Journal of Structural Integrity and Maintenance*, Vol. 1, No. 1, 2016, pp. 22–34.
[17] Sethi, S. and B. C. Ray. Experimental study on the mechanical behavior and microstructural assessment of Kevlar/epoxy composites at liquid nitrogen temperature. *Journal of the Mechanical Behavior of Materials*, Vol. 23, No. 3–4, 2014, pp. 95–100.
[18] Akbarian, M., S. Hassanzadeh, and M. Moghri. Short Twaron aramid fiber reinforced thermoplastic polyurethane. *Polymers for Advanced Technologies*, Vol. 19, 2008, pp. 1894–1900.
[19] Product data sheet, version 05/2017, Biresin® CR80 composite resin systém.
[20] Unwin, A. P., P. J. Hine, I. M. Ward, M. Fujita, E. Tanaka, and A. A. Gusev. Escaping the Ashby limit for mechanical damping/stiffness trade-off using a constrained high internal friction interfacial layer. *Scientific Reports*, Vol. 8, 2018, id. 2454.
[21] Kopal, I., M. Harničárová, J. Valíček, and M. Kušnerová. Modeling the temperature dependence of dynamic mechanical properties and visco-elastic behavior of thermoplastic polyurethane using artificial neural network. *Polymers*, Vol. 9, 2017, id. 519.
[22] Martínez-Hernández, A. L., C. M. Velasco-Santos, and V. M. de-Icaza Castaño. Dynamical–mechanical and thermal analysis of polymeric composites reinforced with keratin biofibers from chicken feathers. *Composites Part B: Engineering*, Vol. 38, No. 3, 2007, pp. 405–410.
[23] Em-Udom, J. and N. Pisutha-Armond. Prediction of mechanical-hysteresis behavior and complex moduli using the phase field crystal method with modified pressure controlled dynamic equation. *Materials Research Express*, Vol. 7, 2020, id. 015326.
[24] Gupta, M. K. and A. Bharti. Natural fibre reinforced polymer composites: A review on dynamic mechanical properties. *Current Trends in Fashion Technology and Textile Engineering*, Vol. 1, No. 3, 2017, id. 555563.
[25] Andreopoulos, A. G. and P. A. Tarantili. Study of the off-axis properties of composites reinforced with ultra high modulus polyethylene fibres. *European Polymer Journal*, Vol. 35, No. 6, 1999, pp. 1123–1131.
[26] Patidar, D., S. Agrawal, and N. S. Saxena. Storage modulus and glass transition behaviour of CdS/PMMA nanocomposites. *Journal of Experimental Nanoscience*, Vol. 6, No. 4, 2011, pp. 441–449,
[27] Advanced composites solutions high performance epoxy and polyurethane systems, Sika®, Issue February 2019.
[28] Bazan, P., P. Nosal, B. Kozub, and S. Kuciel. Biobased polyethylene hybrid composites with natural fiber: Mechanical, thermal properties, and micromechanics. *Materials*, Vol. 13, 2020, id. 2967.
[29] Bazli, M. and M. Abolfazli. Mechanical properties of fibre reinforced polymers under elevated temperatures: An overview. *Polymers*, Vol. 12, No. 11, 2020, id. 2600.
[30] Bergström, J. *Mechanics of solid polymers*. William Andrew Publishing, USA, 2015.
[31] Newman, A. and G. Zografi. Commentary: Considerations in the measurement of glass transition temperatures of pharmaceutical amorphous solids. *AAPS PharmSciTech*, Vol. 21, 2020, pp. 26.
[32] Lettieri, M. and M. Frigione. Effects of humid environment on thermal and mechanical properties of a cold-curing structural epoxy adhesive. *Construction and Building Materials*, Vol. 30, 2012, pp. 753–760
[33] Maljaee, H., B. Ghiassi, and P. B. Lourenço. Effect of synergistic environmental conditions on thermal properties of a cold curing epoxy resin. *Composites Part B: Engineering*, Vol. 113, 2017, pp. 152–163.